Earthquake early warning for southern Iberia: A *P* wave threshold-based approach

M. Carranza,[1] E. Buforn,[1] S. Colombelli,[2] and A. Zollo[2]

Received 12 July 2013; revised 22 August 2013; accepted 23 August 2013.

[1] The south of the Iberian Peninsula is a region in which large, damaging earthquakes occur separated by long time intervals. An example was the great 1755 Lisbon earthquake (intensity $I_{max} = X$) which occurred SW of San Vicente Cape (SW Iberian Peninsula). Due to this risk of damaging earthquakes, the implementation of Earthquake Early Warning System (EEWS) technologies is of considerable interest. With the aim of investigating the feasibility of an EEWS in this region of the Iberian Peninsula, empirical scaling relationships have been derived between the early warning parameters and the earthquake size and/or its potential damaging effects for this region. An appropriate and suitable strategy is proposed for an EEWS in the SW Iberian Peninsula, which takes into account the limitations of the existing seismological networks. **Citation:** Carranza, M., E. Buforn, S. Colombelli, and A. Zollo (2013), Earthquake early warning for southern Iberia: A *P* wave threshold-based approach, *Geophys. Res. Lett.*, *40*, doi:10.1002/grl.50903.

1. Introduction

[2] The use of an earthquake early warning system (EEWS) is increasingly being seen as of importance to prevent and mitigate the destructive effects of an earthquake. An EEWS is a real-time system able to detect an earthquake in progress, and to provide fast notification of its potential to cause damage in a target area before the destructive waves arrive. Such systems are based on rapid telemetric analysis of data provided by an instrument array deployed in the source and/or target areas. Several countries around the world have already developed EEWS's. Examples are those now satisfactorily operating in Japan [*Hoshiba et al*., 2008], Taiwan [*Wu and Zhao*, 2006], and Mexico [*Espinosa-Aranda et al*., 2009]. Specifically, the EEWS from the JMA (Japan Meteorological Agency) is giving service to general public since 2007. Other systems are currently being tested or are under development – in California, Turkey, Romania, China, and southern Italy (see overview by *Allen et al*. [2009]). Most are designed as either regional or on-site systems. In the regional approach, the earthquake's location and magnitude are estimated using the early portion of recorded signals. The peak ground motion at distant sites is then predicted using an empirical ground-motion prediction equation. In an on-site configuration, the earthquake early warning (EEW) parameters measured in the very first seconds of the *P* wave are used to predict the final peak ground motion at the same site. A recent methodological development has been to integrate the two strategies so as to estimate a Potential Damage Zone (PDZ) for the impending earthquake (i.e., the area in which most of the damage is expected to occur) and to define local alert levels [*Zollo et al*., 2010]. An alternative approach is "front detection," which consists in the installation of an array of seismic sensors between the potential source area and the target area. Such a system requires prior knowledge of the possible earthquake sources, but, depending on their distance from the target area, it can then provide quite long warning times (i.e., tens of seconds). An example of a front detection system is the Seismic Alert System (SAS) for Mexico City [*Espinosa-Aranda et al*., 1995] which has an array of sensors along the coast designed to detect earthquakes from the adjacent subduction zone and to transmit the warning to Mexico City.

[3] Generally, two EEW parameters are determined from the early portion of the *P* wave signal: the peak ground displacement (P_d) and the predominant period (τ_c). These observed quantities are related empirically to the magnitude and to the Peak Ground Velocity (PGV) [*Wu and Kanamori*, 2005a]. Recently, *Colombelli et al*. [2012] have discussed the effectiveness of these parameters for the 2011 Tohoku-Oki earthquake, suggesting the use of enlarged *P* wave time windows for such large earthquakes. In the present work, we determined the EEW parameters P_d and τ_c from a database of earthquakes that occurred in the south of the Iberian Peninsula. The objective is to obtain the specific empirical relationships of these parameters with the final magnitude of the earthquake. The Iberian Peninsula is undergoing a NNW-SSE horizontal compression resulting from the convergence of the Eurasian and African plates. The region situated at the plate boundary is an area of occurrence of large earthquakes with a long separation in time [*Buforn et al*., 1988], and in the 20th century, it was seismically very quiet as compared to other historical periods. The area of San Vicente Cape (Figure 1a) has generated large shocks, including the damaging 1755 Lisbon earthquake ($I_{max} = X$), and, more recently, the Ms = 8.1 1969 S. Vicente Cape earthquake, both of which generated tsunamis. Moderate-to-strong earthquakes have also occurred in the Gulf of Cádiz (Ms = 6.5 1964 event). But in this area even smaller magnitude earthquakes can cause considerable panic and fear among the population since they are felt over an extensive region, as was the case with the December 2009 earthquake ($M_w = 5.5$) which was felt over a major part of the SW of the Iberian Peninsula. The occurrence of the 1755 Lisbon

Additional supporting information may be found in the online version of this article.

[1]Dept. Geofísica y Meteorología, Universidad Complutense, Madrid, Spain.

[2]Dept. Physics, Università Federico II, Naples, Italy.

Corresponding author: M. Carranza, Dept. Geofísica y Meteorología. Universidad Complutense, Madrid, Spain. (macarran@ucm.es)

0094-8276/13/10.1002/grl.50903

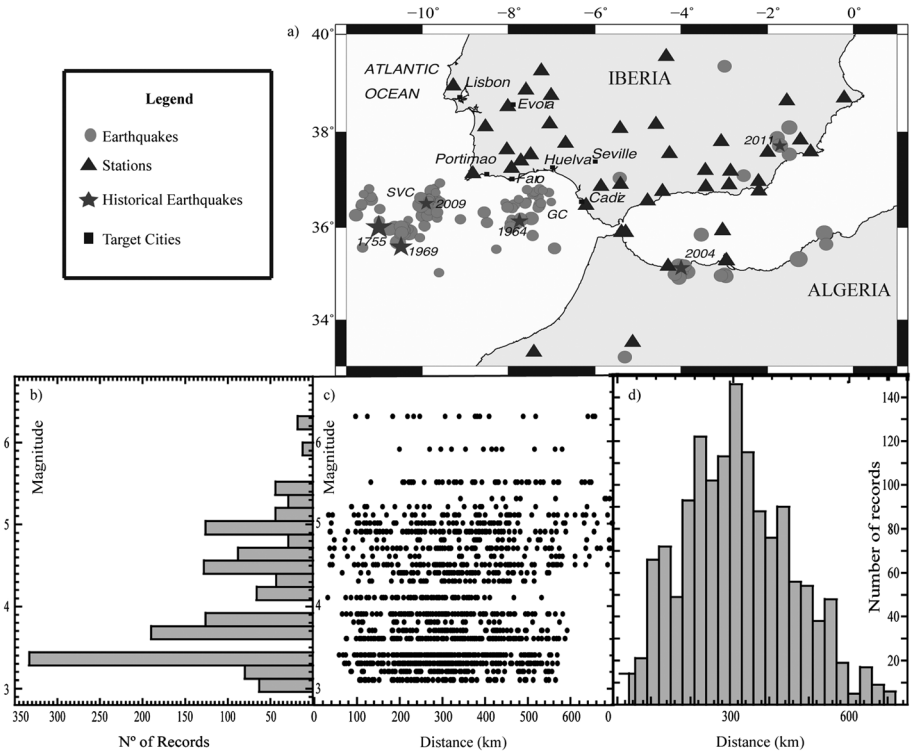

Figure 1. (a) Distribution of the epicenters (gray circles) used in this study. Black triangles are the broadband stations considered. Stars are the 1755, 1964, 1969, 2004, 2009, and 2011 epicenters. The San Vicente Cape (SVC) and Gulf of Cadiz (GC) regions are highlighted. (b) Distribution of earthquakes as a function of magnitude. (c) Scatter plot of earthquakes as a function of hypocentral distance and magnitude. (d) Distribution of the records as a function of hypocentral distance.

earthquake is a good reason to study the feasibility of and EEWS in this area. The level of vulnerability at SW Iberian coast has been increased by the large urbanistic development and this make us more and more involved in investigating and assessing the risk of very rare, large events.

2. Database and Methods

[4] We first selected 94 earthquakes from the IGN (Instituto Geográfico Nacional) catalogue that had occurred in the period 2006–2011 with magnitudes ranging from 3.8 to 5.9, and located in the S. Vicente Cape-Gulf of Cadiz area. Due to the lack of earthquakes with magnitudes greater than 6.0 and epicentral distances less than 200 km, the database was extended with an additional 25 events ($M_w > 4.5$) located in SE Iberia and North of Africa (Figure 1a). We analysed a selection of 1416 three-component velocity records at regional distances (30–700 km) by 41 widely spread real-time transmission broadband seismic stations of the IGN, Western Mediterranean (WM), and Portuguese National (IP) networks (Figure 1a). The distribution of these records as a function of epicentral distance and magnitude is shown in Figures 1b, 1c, and 1d. The maximum magnitude in the database is $M_w = 6.3$ corresponding to the 2004 Al-Hoceima earthquake, but most of the records correspond to events with magnitudes smaller than $M_w = 4.0$. The epicentral distances range between 30 and 700 km, with most of the data concentrated between 200 and 400 km.

[5] The records were first corrected by removing the mean value and linear trend. The *P*- and *S* wave pickings were manually checked on the unfiltered vertical and horizontal components, respectively. To avoid the inclusion of very noisy data, which can result in anomalous parameter values being determined, we computed the signal-to-noise ratio by comparing the maximum signal amplitude (in a 5 s window after *P* wave arrival) with the pre-event noise level (in a 5 s window before *P* wave arrival) on the vertical component of each velocity record. We selected for subsequent analysis only those records with a signal-to-noise ratio greater than five, a value that excludes very noisy data without overrestricting the database. With this criterion, the number of records was reduced to 544. The parameter τ_c can be considered as representing the average period of the *P* wave signal [*Wu and Kanamori*, 2005b]. Its logarithm is linearly related to the magnitude of the event. It is defined as

$$\tau_c = 2\pi\sqrt{\int_0^{\tau_0} u^2(t)dt / \int_0^{\tau_0} v^2(t)dt} \quad (1)$$

where *u* and *v* are the ground displacement and velocity, respectively, computed over a time window starting at the *P* wave onset time with a duration equal to τ_0 (usually a 3 s window is used). For the determination of τ_c, we used the vertical component of the unfiltered broadband velocity records. To obtain the displacement, we integrated the velocity records and applied a high-pass Butterworth filter, with corner frequency at 0.075 Hz and two poles, to remove the low frequencies introduced by the integration process. For the sake of uniformity with the literature, we used a time window τ_0 equal to 3 s. The parameter P_d is defined as the peak displacement of the first three seconds of the *P* wave signal. This parameter is related to the earthquake magnitude (M) and the hypocentral distance (R) [e.g., *Zollo et al.*, 2006] through the standard attenuation expression

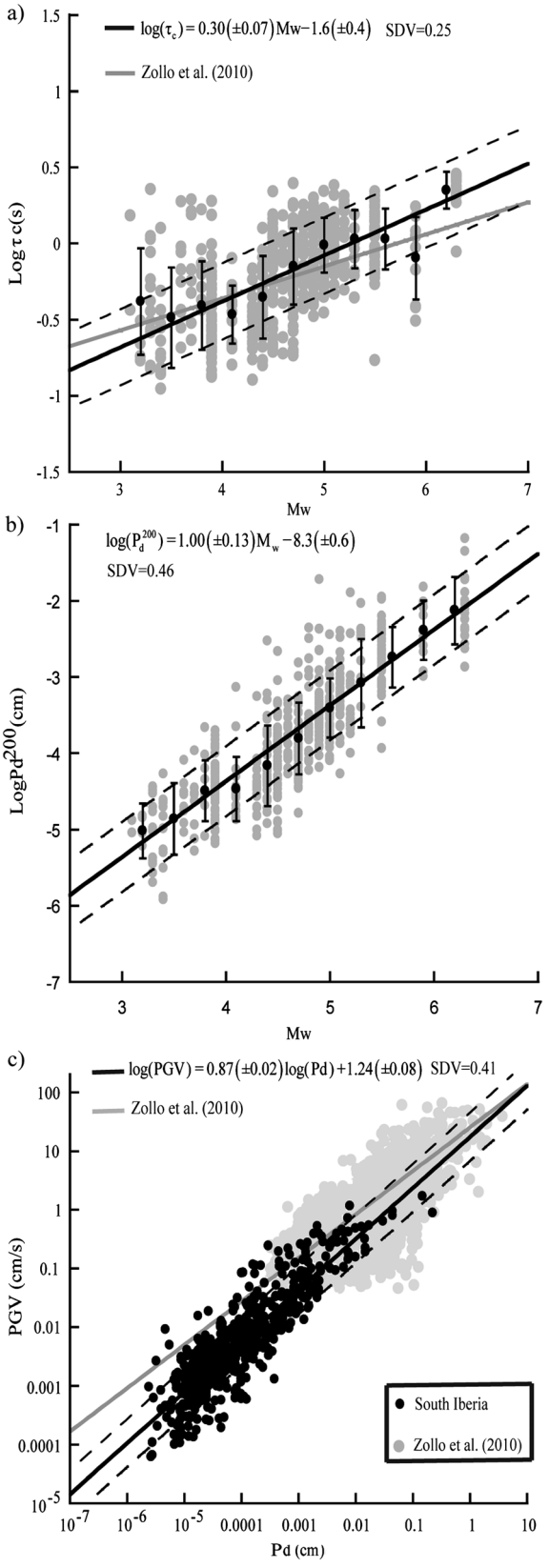

Figure 2

$$\log(P_d) = A + B*M + C*\log(R) \quad (2)$$

where A, B, and C are constants to be determined by a multivariate linear regression analysis of the specific region's data. Once the P_d parameter has been normalized to a reference distance, thus correcting for the geometrical spreading effect, one can obtain a log-linear relationship with M. P_d was estimated as the maximum value of the displacement within the 3-s *P* wave window after integrating the vertical component of the velocity records and applying the high-pass filter (Butterworth, 0.075 Hz corner frequency). The high-pass filtered, *P* wave peak displacement can also be related to the final PGV value at the station [*Wu and Kanamori*, 2005a]. This value was determined as the maximum velocity of the two unfiltered horizontal components of the velocity records. A relevant question in our data set is what type of magnitude to consider. The empirical scaling laws obtained for other regions are generally calibrated using the moment magnitude (M_w) [*Zollo et al*., 2010] or the local magnitude (M_l) [*Wu and Kanamori*, 2005a]. Three types of magnitude are listed in the IGN catalogue for the studied period. To homogenize the magnitudes of our data set, we used the preliminary IGN relationships [*Cabañas et al*., 2012] to convert the different magnitudes to the M_w magnitude. After selection, we obtain an event data set with magnitude ranging from 3.1 to 6.3. The uncertainty on M_w due to the conversion is taken into account when binning the data in magnitude intervals, as detailed in the following section.

3. Application and Results

[6] We applied the above procedure to compute the two EEW parameters. Figure 2a is a plot of the logarithm of τ_c as a function of the moment magnitude (M_w). The linear regression line was obtained for the means of τ_c in bins of $\Delta M_w = 0.3$ width, and weighted by the standard deviation of each bin. Its expression is

$$\log(\tau_c) = 0.30(\pm 0.07)M_w - 1.6(\pm 0.4) \quad (3)$$

where τ_c is in seconds, and M_w is the moment magnitude computed by the aforementioned empirical relationships. The average τ_c values generally increase with the magnitude of the event, and most of the data lie within 1σ error bounds.

Figure 2. (a) Logarithm of the period (τ_c) versus the moment magnitude for southern Iberia. Black dots represent the average value for each bin ($\Delta M = 0.3$) and are plotted with their corresponding standard deviations. The continuous black line represents the best fit for the means, and the dashed lines are the ±1σ standard error bounds. The continuous gray line represents the correlation reported by *Zollo et al*. [2010]. (b) Logarithm of P_d parameter reduced to a standard distance of 200 km, versus the moment magnitude for southern Iberia (gray dots). Black dots represent the mean value for each bin ($\Delta M = 0.3$) and are plotted with their corresponding standard deviations. The solid line is the best fit, and the dashed lines are the ±1σ standard error bounds. (c) Peak ground velocity (PGV) versus the peak displacement (P_d) displayed on a logarithmic scale. The black dots represent data from southern Iberia. Gray dots represent data from earthquakes of Japan, Taiwan, and Italy [*Zollo et al*., 2010]. The solid black line is the best fit and the dashed lines represent the ±1σ standard error bounds. The continuous gray line represents the correlation reported by *Zollo et al*. [2010].

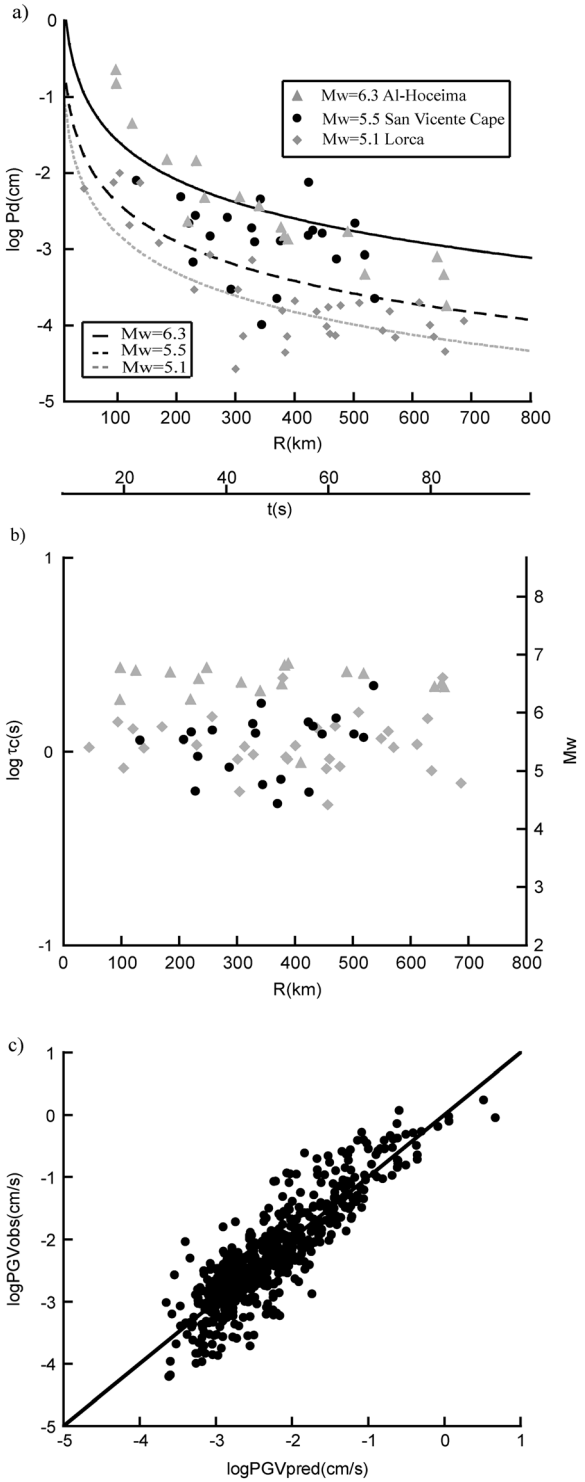

Figure 3. Time from the origin of the parameter estimation at various stations for the Al-Hoceima 2004 ($M_w = 6.3$, gray triangles), Lorca 2011 ($M_w = 5.1$, gray diamonds), and S. Vicente Cape 2009 ($M_w = 5.5$, black dots) earthquakes. (a) Log-linear plot of the initial peak displacement versus distance. (b) Logarithm of the τ_c parameter versus the distance of the station. The right axis shows the expected M_w magnitude given by equation 3. A timeline is shown between Figures 3a and 3b representing the time from earthquake's origin plus 3 s of time window needed to obtain the parameters. (c) Predicted PGV (PGVpred) versus observed PGV (PGVobs). Black line shows the 1:1 line.

The figure also shows (solid gray) the regression line found by *Zollo et al*. [2010] with data from Taiwan, Japan, and the south of Italy.

[7] With the same approach, we applied a linear regression analysis to determine the coefficients of equation 2 that relate the initial peak displacement (P_d) to the hypocentral distance (R) and moment magnitude (M_w), finding

$$\log(P_d) = 1.02(\pm 0.03)M_w - 1.70(\pm 0.08)\log(R) - 4.6(\pm 0.2) \quad (4)$$

where P_d is in centimeters, and R is in kilometers. This equation allows all the values of P_d to be normalized to a reference distance of 200 km, chosen since it corresponds approximately to the nearest epicentral distance available for the events located in the Lisbon 1755 earthquake source region. Figure 2b shows the normalized peak displacement (henceforth P_d^{200}) as a function of the moment magnitude (M_w). The correlation equation computed with the mean of the binned data ($\Delta M_w = 0.3$ bins) and weighted by the standard deviation of each mean value is

$$\log(P_d^{200}) = 1.00(\pm 0.13)M_w - 8.3(\pm 0.6) \quad (5)$$

where P_d^{200} is given by equation 4 and is expressed in centimeters. As was the case for τ_c, the mean P_d^{200} values are strongly correlated with the magnitude, and lie within the error bounds (Figure 2b). Finally, we correlated P_d measured in the first 3 s of the *P* wave signal with the PGV determined from the entire seismogram. In Figure 2c, the black dots are the present results, and the gray dots are the results reported by *Zollo et al*. [2010] who calibrated the scaling relationships using an independent data set of earthquakes from Taiwan, Japan, and Italy in the magnitude range $4 < M < 8.3$ and at distances between 0 and 60 km. The calculated regression line for the southern Iberia data was

$$\log(PGV) = 0.87(\pm 0.02)\log(P_d) + 1.24(\pm 0.08) \quad (6)$$

where the units of PGV are centimeters per second and of P_d are centimeters. To validate the results, we selected three events in our data set: the 2004 Al-Hoceima (N Morocco, $M_w = 6.3$), the 2009 S. Vicente Cape ($M_w = 5.5$), and the 2011 Lorca (SE Spain $M_w = 5.1$) earthquakes. Figures 3a and 3b show the evolution with time and distance of the observed EEW parameters (P_d and τ_c) for these three earthquakes at different stations. The time axis represents the theoretical time at which P_d and τ_c measurements are available at any station (including the *P* wave arrival time at the station plus the 3 s time window of computation). As expected, for all the cases, P_d shows a general decrease with increasing distance, due to the combined effects of geometrical and anelastic attenuation (Figure 3a). The expected values of the magnitudes of these three earthquakes estimated with equation 4 are also plotted in Figure 3a. They agree well with the observed data distribution. In Figure 3b, we can observe the evolution of the measured τ_c with distance/time from the earthquake origin. The plot shows that τ_c values do not show any significant dependence with distance up to 700 km. The right axes of Figure 3b, shows the M_w value derived from equation 3. For the Al-Hoceima 2004 earthquake (Figure 3b, gray triangles), equation 3 predicts M_w values from 5.1 to 6.8 with a mean value of 6.5 ± 0.3. This is consistent within the uncertainties with the value of $M_w = 6.3$ estimated by other methods. For both the 2009 and the 2011 shocks (black dots and gray diamonds, respectively), despite

the greater scatter of the data, the estimated mean value M_w 5.4 ± 0.5 is consistent within the uncertainties with the values $M_w = 5.5$ and 5.1 given in the catalogue.

[8] As a further test, we computed the error in the estimation of PGV. To this end, we plotted in Figure 3c the observed PGV versus the predicted PGV given by equation 6 and found that data are distributed close to the line with slope 1, thus confirming the robustness of P_d as a predictor of PGV.

4. A Conceptual Idea of an EEWS for Southern Iberia

[9] In the preceding sections, we have described the use of velocity records for earthquakes that occurred in the south of the Iberian Peninsula to derive empirical scaling relationships between EEW parameters (τ_c, P_d) and magnitude or peak ground velocity (PGV), which is related to the potential damage of the earthquake. This case of study of the Iberian region is a good test of EEW methodologies due to the small magnitude range (3.1 to 6.3) and the poor station coverage at small epicentral distances. Despite the limitations of the data set used, our data distribution was found to be consistent with the empirical regression lines obtained by *Zollo et al*. [2010] for strong motion data from Japan, Taiwan, and Central Italy for the same magnitude range (Figure 2a). In addition, the comparison of the present results for the P_d versus PGV relationship with those obtained by *Zollo et al*. [2010] showed good agreement between the two data sets and similar scaling relationships (Figure 2c). This is confirmation that the correlation between P_d and PGV is robust even at large hypocentral distances (in our case mostly greater than 200 km) and lower magnitudes (from 3.1 to 6.3), and that it is independent of the effects of the tectonic region, source, attenuation, or site which may influence the scatter of the data around the mean trends. The use of τ_c and P_d measured within few seconds of the *P* wave signal is widely adopted for early warning and it has been shown to provide reliable magnitude estimates for events with magnitudes up to 7 [*Allen et al*., 2009]. By analysing the strong motion data of the M 9, 2011 Tohoku-Oki event, *Colombelli et al*. [2012] showed that a *P* wave time window larger than 3 s is needed to correctly estimate the magnitudes of very large earthquakes ($M > 8$). In our region of study, the 1755 Lisbon earthquake can be considered a mega-earthquake, and other events of magnitude greater than 8 are expected [*Buforn et al*., 1988]. Since our data set does not include any such large events, we did not evaluate the effect of increasing the size of the *P* wave time window. However, the use of an evolutionary EEWS with enlarging time windows as more records are available is an important issue to be further studied since large earthquakes are indeed expected to occur in the South Iberia region.

[10] The principal motivation behind the present study has been the great interest in mitigating the potential effects of seismic risk in the S. Vicente Cape area. The present distribution of real-time, broadband transmission stations in SW Iberia is very sparse and provides a poor azimuthal coverage (Figure 1a). This situation makes it difficult to obtain an early and reliable location of the epicenter, and the poor azimuthal and distance coverage makes depth estimates likely to be erroneous, although such uncertainties in depth would have a negligible effect on distance estimates in this region. A threshold-based approach, which would not require real-time location of the quake, might therefore be the best option for an EEWS in SW Iberia. As an example of the practical application of the present results for the implementation of such an EEWS, we determined different threshold values of the P_d and τ_c parameters for three magnitudes ($M = 6$, 7, and 8). We assumed the epicenter to be located in the same source region as that of the 1755 Lisbon earthquake, with the closest distance to the coast being about 200 km. For each magnitude, we computed the expected PGV using the ground motion prediction equation (GMPE) obtained by *Akkar and Bommer* [2010]. We then converted the expected PGV into a P_d threshold value using equation 6 and taking a 1 standard error limit. For the τ_c threshold, we used equation 3, again taking into account the standard deviation (Table A1 of the supplemental material). The main advantage of this threshold-based approach is that the potential damaging effects of an offshore earthquake can be rapidly evaluated by the real-time analysis of data from coastal stations without any need for accurate estimation of the earthquake's location. While the τ_c parameter provides an estimate of the magnitude through equation 3, the P_d parameter provides an estimate of the PGV amplitude through equation 6 and hence of the intensity at the recording site. When the threshold value is surpassed at a certain number of stations, a rapid earthquake alert can be issued, and the coastal areas and inland regions of the Iberian Peninsula notified. Even considering the large scatter of data in Figures 2a and 2b, the magnitude estimation through the empirical regression model is more and more refined when the number of observations increases. For this reason, robust magnitude estimation should be always based on more than a single station measurement [*Satriano et al*., 2010]. With this aim, we computed the differences in lead times at several Portuguese and Spanish target cities (see Table A2 at supplemental material), as a function of the number of stations used to issue an alert. Assuming the present network configuration and a virtual earthquake colocated with that of Lisbon 1755, we computed the lead time (i.e., the time between the issue of the alert and the arrival of the *S* wave) for various target cities (Figure 1a), and for three cases—assuming a minimum of 1, 5, or 10 triggered stations needed for the alert to be issued. The complete list of stations considered and their corresponding alert times is provided in Table A3 of the Supporting Material. The more triggered stations required for the alert to be issued, the smaller the lead times are for the target, although the estimation of the potential damage of the impending earthquake will be more reliable given the contemporary observation of values over the threshold by several close-by stations. With the current network configuration, a minimum number of 10 stations needed to trigger the alert would mean that Portimao would be within the blind zone that could not be alerted. Only 5 s would be available at Faro, 21 s at Lisbon and 46 s at the farthest city, Seville. Early *S* wave peak displacement amplitudes can be also used for early warning at in-land target cities of the Iberian Peninsula [e.g., *Lancieri and Zollo*, 2008]. In this case, the lead time is reduced by 15 s relative to the 10 stations *P* wave system. It needs to be borne in mind that, while the proposed *P* wave threshold-based EEWS can rapidly issue an alert for large seismic events occurring offshore of the Iberian Peninsula, it cannot provide an estimate of the lead time. For this, a reliable estimate is needed of the quake's location. The actual network configuration, possibly improved with more coastal stations, can provide

accurate estimations of back azimuth, by using array techniques for earthquake location. However, the accuracy on epicenter and depth determination could be poor for offshore events. A suitable event location technique could be the RTLoc (Real-Time Location) method of *Satriano et al*. [2008] implemented in the EEW software platform PRESTo [*Satriano et al*., 2010]. Alternatively, an approximate source-to-receiver distance can be estimated by solving the system of equations for the unknown parameter log R, given the observed P_d and τ_c at the closest coastal sites (equations 3 and 4). The histogram of the prediction error against log R (Fig. A1 of the Supporting Material) shows that distance residuals are log-normally distributed around zero (with a ±0.5 standard deviation). The combined use of equations 3 and 4 can therefore provide both a reliable (although approximate) estimate of the epicentral distance and useful information on the expected lead time at the recording site. This information can then be refined when more data become available from close-by stations to provide an average value of the distance. This suggests the advisability of the future dense deployment of seismic arrays along the Atlantic coast of the Iberian Peninsula to form an early warning "front-detection" network [*Allen et al*., 2009]. Such a network could provide rapid and reliable alerts together with information about the magnitude, distance, and potential damaging effects of the event. In our vision, the first primary piece of information provided by the envisaged front-detection EWS for Iberian Peninsula should be a threshold-based one, which does not depend on distance and/or magnitude determination of the event. However, since the first *P* wave arrival times are collected at the real-time network, they could be used to infer additional and complementary information about the possible location and magnitude, although with a large uncertainty.

[11] **Acknowledgments.** The authors wish especially to thank Luis Cabañas of the IGN (Spain) for constructive discussions about the magnitude conversion equations. This work was financially supported by Spain's Ministerio de Educación y Ciencia CGL2010-19803-C03-01 project, by the NERA project which financed a three-month stay at the RISSC Laboratory (University of Naples, Italy), and by the EU-FP7 project framework.

[12] The Editor thanks Gilead Wurman and an anonymous reviewer for their assistance in evaluating this manuscript.

References

Akkar, S., and J. J. Bommer (2010), Empirical equations for the prediction of PGA, PGV and spectral accelerations in Europe, the Mediterranean region and the Middle East, *Seism. Res. Lett.*, *81*, 195–206.

Allen, R. M., P. Gasparini, O. Kamigaichi, and M. Bose (2009), The Status of Earthquake Early Warning around the World: An Introductory Overview, *Seism. Res. Lett.*, *80*(5), 682–693.

Buforn, E., A. Udías, and M. A. Colombás (1988), Seismicity, source mechanisms and seismotectonics of the Azores-Gibraltar plate boundary, *Tectonophysics*, *152*, 89–118.

Cabañas, L., A. Rivas, J. M. Martínez-Solares, J. Gaspar-Escribano, B. Benito, R. Antón, and S. Ruiz-Barajas (2012), Preparación y homogeneización de un catálogo sísmico para la evaluación de la peligrosidad sísmica en España, *7ª AHPGG Donostia*, *25-29 june 2012*.

Colombelli, S., A. Zollo, G. Festa, and H. Kanamori (2012), Early magnitude and potential damage zone estimates for the great M_w 9 Tohoku-Oki earthquake, *Geophys. Res. Lett. 39*, L22306, doi:10.1029/2012GL053923.

Espinosa-Aranda, J. M., A. Jiménez, G. Ibarrola, F. Alcantar, A. Aguilar, M. Inostrosa, and S. Maldonado (1995), Mexico City Seismic Alert System, *Seism. Res. Lett.*, *66*(6), 42–52.

Espinosa-Aranda, J. M., A. Cuellar, A. Garcia, G. Ibarrola, R. Islas, S. Maldonado, and F. H. Rodriguez (2009), Evolution of the Mexican Seismic Alert System (SASMEX), *Seism. Res. Lett.*, *80*, 694–706.

Hoshiba, M., O. Kamigaichi, M. Saito, S. Tsukada, and N. Hamada (2008), Earthquake early warning starts nationwide in Japan, *EOS Trans. AGU*, *89*, 73–74.

Lancieri, M., and A. Zollo (2008), A Bayesian approach to the real-time estimation of magnitude from the early *P* and *S* wave displacement peaks, *J. Geophys. Res.*, *113*, B12302, doi:10.1029/2007JB005386.

Satriano, C., A. Lomax, and A. Zollo (2008), Real-time evolutionary earthquake location for seismic early warning, *Bull. Seism. Soc. Am.*, *98*, 1482–1494.

Satriano, C., L. Elia, C. Martino, M. Lancieri, A. Zollo, and G. Iannaccone (2010), PRESTo, the earthquake early warning system for Southern Italy: Concepts, capabilities and future perspectives, *Soil Dynam. Earthquake*, *31*, 137–153.

Wu, Y.-M., and H. Kanamori (2005a), Experiment on an onsite early warning method for the Taiwan early warning system, *Bull. Seism. Soc. Am.*, *95*, 347–353.

Wu, Y.-M., and H. Kanamori (2005b), Rapid assessment of damage potential of earthquakes in Taiwan from the beginning of P-waves, *Bull. Seism. Soc. Am.*, *95*, 1181–1185.

Wu, Y.-M., and L. Zhao (2006), Magnitude estimation using the first three seconds P-wave amplitude in earthquake early warning, *Geophys. Res. Lett.*, *33*, L16312, doi:10.1029/2006GL026871.

Zollo, A., M. Lancieri, and S. Nielsen (2006), Earthquake magnitude estimation from peak amplitudes of very early seismic signals on strong motion records, *Geophys. Res. Lett.*, *33*, L23312, doi:10.1029/2006GL027795.

Zollo, A., O. Amoroso, M. Lancieri, Y.-M. Wu, and H. Kanamori (2010), A Threshold-based Earthquake Early Warning using dense accelerometer networks, *Geophys. J. Int.*, *183*, 963–974.